

UC Berkeley

UC Berkeley Previously Published Works

Title

Typical readout durations in spiral cine DENSE yield blurred images and underestimate cardiac strains at both 3.0 T and 1.5 T

Permalink

<https://escholarship.org/uc/item/5vv3v9mq>

Authors

Wehner, Gregory J
Suever, Jonathan D
Fielden, Samuel W
et al.

Publication Date

2018-12-01

DOI

10.1016/j.mri.2018.08.003

Peer reviewed



Published in final edited form as:

Magn Reson Imaging. 2018 December ; 54: 90–100. doi:10.1016/j.mri.2018.08.003.

Typical Readout Durations in Spiral Cine DENSE Yield Blurred Images and Underestimate Cardiac Strains at Both 3.0 T and 1.5 T

Gregory J. Wehner, PhD^a, Jonathan D. Suever, PhD^b, Samuel W. Fielden, PhD^{b,c}, David K. Powell, PhD^a, Sean M. Hamlet, PhD^d, Moriel H. Vandsburger, PhD^{a,e}, Christopher M. Haggerty, PhD^b, Xiaodong Zhong, PhD^f, Brandon K. Fornwalt, MD, PhD^{b,g}

Gregory J. Wehner: wehnergj@gmail.com; Jonathan D. Suever: suever@gatech.edu; Samuel W. Fielden: sfielden@geisinger.edu; David K. Powell: dkpowe00@mri.uky.edu; Sean M. Hamlet: seanmhamlet@gmail.com; Moriel H. Vandsburger: moriel@berkeley.edu; Christopher M. Haggerty: chaggerty3@gatech.edu; Xiaodong Zhong: xiaodong.zhong@siemens.com; Brandon K. Fornwalt: bkf@gatech.edu

^aDepartment of Biomedical Engineering, University of Kentucky, Lexington, KY, United States

^bDepartment of Imaging Science and Innovation, Geisinger, Danville, PA, United States

^cDepartment of Medical & Health Physics, Geisinger, Danville, PA, United States

^dDepartment of Electrical Engineering, University of Kentucky, Lexington, KY, United States

^eDepartment of Physiology, University of Kentucky, Lexington, KY, United States

^fMR R&D Collaborations, Siemens Healthcare, Atlanta, GA, United States

^gDepartment of Radiology, Geisinger, Danville, PA, United States

Abstract

Address for correspondence Brandon K Fornwalt, bkf@gatech.edu, Center for Health Research, Geisinger Clinic, 100 North Academy Avenue, Danville, PA 17822-4400, (570) 214-5478.

Authors' Contributions

GW analyzed and collected data, assisted with study conception, design and implementation, and drafted the manuscript. JS assisted with study conception and design, data analysis, and critical revision of the manuscript. SF assisted with data analysis and critical revision of the manuscript. DP and SH assisted with data collection and critical revision of the manuscript. MV, CH and XZ assisted with critical revision of the manuscript. BF assisted with study conception and design, and drafting and critical revision of the manuscript. All authors read and approved the final manuscript.

Competing Interests

Dr. Zhong is a Siemens employee. The authors otherwise have no relevant conflicts of interest to disclose.

Declarations

Ethics Approval and Consent to Participate

The study was approved by Institutional Review Board at the University of Kentucky. All participants provided written and informed consent.

Consent for Publication

Not applicable.

Availability of Data and Material

The datasets generated and/or analyzed during the current study are available on reasonable request with approval of the corresponding author.

Publisher's Disclaimer: This is a PDF file of an unedited manuscript that has been accepted for publication. As a service to our customers we are providing this early version of the manuscript. The manuscript will undergo copyediting, typesetting, and review of the resulting proof before it is published in its final citable form. Please note that during the production process errors may be discovered which could affect the content, and all legal disclaimers that apply to the journal pertain.

Introduction: Displacement encoding with stimulated echoes (DENSE) is a phase contrast technique that encodes tissue displacement into phase images, which are typically processed into measures of cardiac function such as strains. For improved signal to noise ratio and spatiotemporal resolution, DENSE is often acquired with a spiral readout using an 11.1 ms readout duration. However, long spiral readout durations are prone to blurring due to common phenomena such as off-resonance and T2* decay, which may alter the resulting quantifications of strain. We hypothesized that longer readout durations would reduce image quality and underestimate cardiac strains at both 3.0 T and 1.5 T and that using short readout durations could overcome these limitations.

Material and Methods: Computational simulations were performed to investigate the relationship between off-resonance and T2* decay, the spiral cine DENSE readout duration, and measured radial and circumferential strain. Five healthy participants subsequently underwent 2D spiral cine DENSE at both 3.0 T and 1.5 T with several different readout durations 11.1 ms and shorter. Pearson correlations were used to assess the relationship between cardiac strains and the spiral readout duration.

Results: Simulations demonstrated that long readout durations combined with off-resonance and T2* decay yield blurred images and underestimate strains. With the typical 11.1 ms DENSE readout, blurring was present in the anterior and lateral left ventricular segments of participants and was markedly improved with shorter readout durations. Radial and circumferential strains from those segments were significantly correlated with the readout duration. Compared to the 1.9 ms readout, the 11.1 ms readout underestimated radial and circumferential strains in those segments at both field strengths by up to 19.6% and 1.5% (absolute), or 42% and 7% (relative), respectively.

Conclusions: Blurring is present in spiral cine DENSE images acquired at both 3.0 T and 1.5 T using the typical 11.1 ms readout duration, which yielded substantially reduced radial strains and mildly reduced circumferential strains. Clinical studies using spiral cine DENSE should consider these limitations, while future technical advances may need to leverage accelerated techniques to improve the robustness and accuracy of the DENSE acquisition rather than focusing solely on reduced acquisition time.

Keywords

DENSE; Spiral; Off-resonance; T2*; Blurring; Strain

1. Introduction

Phase contrast (PC) techniques encode useful information into the phase of the magnetic resonance (MR) signal. The most widely-known such technique is velocity-encoded PCMR [1]. Another useful PC method is Displacement Encoding with Stimulated Echoes (DENSE) [2, 3]. DENSE encodes tissue displacement into the phase of the MR signal, and when applied in the heart, cardiac strain measurements, which are valuable indicators of cardiac function, may be obtained from spatial derivatives of phase images [4, 5]. For improved signal to noise ratio (SNR) and better temporal and spatial resolution, cine DENSE is often acquired with a spiral readout [6–8]. Despite those benefits, spiral readouts are well-known

to be prone to blurring and distortions from sources such as off-resonance and T2* decay [9, 10]. Measured cardiac strains could be particularly affected as blurring would be expected to dampen gradients in the phase images.

The readout duration affects the amount of blurring that is present in spiral imaging. Longer readout durations allow more time for off-resonant spins to accumulate phase and for more T2* decay to occur. Both phenomena result in blurring in spiral imaging [10]. Spiral PCMR techniques have used readout durations between 11.75 and 14 milliseconds [1, 11, 12]. Similarly, two-dimensional (2D) spiral cine DENSE is typically acquired with 6 spiral interleaves [6–8, 13–17] and a readout duration of 11.1 milliseconds. Field strengths of 3.0 T and 1.5 T are both common [7, 8].

While the effects of inhomogeneity and T2* decay are well-characterized for magnitude-reconstructed spiral images, to our knowledge, no systematic evaluation of strain estimates derived from spiral phase images has been performed. Based on the theoretical relationship between blurring and measured strain from DENSE images (Figure 1, details in Supplemental Material), we hypothesized that shorter readout durations would yield improvements in image quality and differences in measured cardiac strains at both 3.0 T and 1.5 T. Furthermore, and also based on the theory developed in Supplemental Material, radial strain was expected to be more dependent on the readout duration than circumferential strain.

2. Materials and Methods

2.1 Computational Simulations

To expand on the illustration of theoretical blurring above, computational simulations of blurring due to off-resonance and T2* decay were performed for different spiral readout durations using MATLAB (The Mathworks Inc, Natick, MA). Specifically, a ring of tissue with un-deformed endocardial and epicardial radii of 24 and 33 mm, respectively, was deformed based on a linear radial displacement gradient such that the endocardial and epicardial borders underwent 7.5 and 3.0 mm of inward radial displacement, respectively, which yielded a 50% fractional thickening that is typical in humans [18]. DENSE images were simulated with the prescribed displacement encoded perfectly into the phase images using the common encoding frequency of 0.10 cycles/mm [16]. The DENSE images had a 2.8×2.8 mm pixel spacing, which is typical for human DENSE imaging. Pixels within the ring of tissue were given a magnitude of unity, while pixels outside the ring had a magnitude of zero.

The k-space of the simulated images was then sampled along uniform density spiral trajectories. To assess different readout durations, the number of spiral interleaves was varied between 6 and 36, which corresponded to readout durations between 11.1 and 1.9 ms (Table 1). For all simulations, the time between readout samples along the spiral interleaves was 4 μ s, and the number of samples was adjusted to maintain the same spatial resolution for all acquisitions. The 6-interleaves acquisition required 2784 samples along each interleaf and had the longest readout duration (11.1 ms). The 36-interleaves acquisition required 480 samples per interleaf and had the shortest readout duration (1.9 ms). Congruent with human

spiral DENSE implementations [7], the spiral interleaves sampled a circular region of k-space within a matrix of 102×102 , which was then zero-padded to 128×128 before reconstruction. During the simulations, global off-resonance frequencies of 0, 30, and 60 Hz as well as global T_2^* constants of infinity, 25, and 5 ms were applied as the spiral interleaves were sampled. The applied values span the range of off-resonance and T_2^* found in healthy participants at 1.5 T [19]. The application of off-resonance (f) and T_2^* decay (T_2^*) resulted in a phase offset and signal decay as a function of time (t) based on

$$s(t) = \int m(\mathbf{r}) e^{-j2\pi\mathbf{k}(t) \cdot \mathbf{r}} e^{-j2\pi f t} e^{-t/T_2^*} d\mathbf{r}$$

(1)

where $m(\mathbf{r})$ is the spatially-distributed signal and $\mathbf{k}(t)$ is the k-space trajectory. There exist many available techniques for off-resonance correction in spiral imaging, but the simple linear correction remains the most widely-used. Because it uses a linear fit to an acquired field map to estimate off-resonance, the actual off-resonance present locally within an image may be significant. In order to get an insight into the resulting strain measurements in areas of high off-resonance, image reconstruction was performed using gridding and without corrections for the applied signal perturbations.

Due to both the inability of spiral interleaves to sample the corners of k-space and the reduced resolution of the spiral sampling (102 vs 128), even perfect sampling along the interleaves followed by perfect gridding would be unable to exactly reconstruct the initial simulated DENSE images. Thus, to obtain an appropriate reference, the Cartesian k-space of the initial simulated images was replaced with zeros for all frequency points that were beyond the circular region sampled by the spiral interleaves. Reference images were then reconstructed via inverse Fourier transform to obtain the best possible images that could result from spiral k-space sampling.

2.2 Participant DENSE Imaging

This protocol was approved by the local Institutional Review Board and five healthy male subjects (age 26 ± 2 years) without history of cardiovascular disease gave informed consent. For each subject, acquisitions took place at both 1.5 T and 3.0 T on an Aera and Trio, respectively (Siemens Healthineers, Erlangen, Germany). The time between acquisitions on the respective Aera versus Trio was 2 days or less for all subjects. A 6-element chest and 24-element spine coil were used at 3.0 T, while 18-element chest and 12-element spine coils were used at 1.5 T. At 3.0 T and before DENSE acquisitions, a cardiac-gated field map was acquired during a breath-hold and used for 2nd order shimming.

Standard localizers were used to plan a four-chamber balanced steady state free precession cine image. A single mid-ventricular short-axis slice was then planned perpendicular to the four-chamber image at end-systole. This short-axis slice was planned parallel to the mitral valve plane and located 50% of the distance between the endocardial LV apex and the mitral

valve plane. With a previously described spiral sequence [7, 8, 20], short-axis 2D cine DENSE images were acquired with the following parameters: 2 spiral interleaves acquired per temporal frame, 360×360 mm² field of view, 128×128 image matrix, 8 mm slice thickness, 1.08 ms echo time, 17 ms repetition time, 20° constant flip angle. Simple encoding [20] with an encoding frequency of 0.10 cycles/mm [16] was used to measure in-plane displacements while through-plane dephasing of 0.08 cycles/mm [21] and CSPAMM [2] were used for echo suppression.

To assess different readout durations in the same manner as the simulations, the short-axis slice was acquired multiple times with readout durations between 1.9 and 11.1 ms. The properties of the spiral interleaves were the same between the human acquisitions and the simulations (Table 1). The order of the DENSE acquisitions was randomized for each subject. During each repetition time, a DENSE encoding gradient, a spiral readout, and spoiling gradients were played out. While acquisitions with shorter spiral readout durations could allow for shorter repetition times and, thus, either better temporal resolution or the acquisition of more than 2 interleaves per heartbeat, there are significant SNR penalties associated with sampling the longitudinal magnetization more frequently. In order to control the temporal resolution and SNR, the repetition time was the same for all acquisitions.

All DENSE acquisitions were performed with fat suppression and a respiratory navigator (acceptance window = ± 3 mm) prescribed at the dome of the liver. Image reconstruction was performed online with gridding and typical linear corrections to partially compensate for off-resonance [8, 22]. The field maps for the linear corrections were acquired during 2 heartbeats within each DENSE acquisition. The structural similarity index (SSIM) was used to quantify image quality of images with different numbers of interleaves [23]. For SSIM calculation, all images from a given subject/field strength session were referenced to the 1.9 ms acquisition for that session after rigid-body registration, as that is the image with the least corruption due to off-resonance or T2* decay.

2.3 DENSE Strain Analysis

Cardiac strains were derived from both the simulated and participant DENSE images using *DENSEanalysis*, an open source software written in MATLAB that is available at <https://github.com/denseanalysis> [24, 25]. The post-processing steps for each cine DENSE slice included manual segmentation of the left ventricular myocardium and semi-automated phase unwrapping to obtain the 2D displacements within each cardiac frame [24]. Following the unwrapping, typical spatial smoothing and temporal fitting of displacements (10th order polynomial) were performed as previously described to obtain smooth trajectories for all tissue points beginning at end-diastole and continuing beyond end-systole [24]. Radial strain and circumferential strain were quantified from the resulting displacement fields for each cardiac frame with the 2D Lagrangian Green finite strain tensor in six circumferential segments throughout the cardiac cycle. Radial strain was defined as positive for thickening while circumferential strain was negative for shortening. To report peak global strains, the curves from the six segments were averaged into a single global curve from which the peak was selected. For circumferential strain both globally and segmentally, the strains were reported at different transmural regions (subendocardial, midwall, and subepicardial).

2.4 Statistics

For each SSIM or peak strain, a Pearson correlation was performed with the mean of the five subjects against the readout duration to determine if the measured value was significantly dependent on the readout duration. An ordinary linear regression between the mean strain and the readout duration was performed to assess the change in measured strain per millisecond of readout duration.

3. Results

3.1 Computational Simulations

As expected, simulations with longer readout durations were more susceptible to blurring from off-resonance and T2* decay (Figure 2A). With an 11.1 ms readout, both off-resonance and T2* decay resulted in visibly-blurred magnitude images. In contrast, the images from a 1.9 ms readout were largely unaffected even in the worst simulated case (60 Hz of off-resonance and a T2* of 5 ms). It is notable that, while the blurring is readily apparent on magnitude images, it is much subtler in phase images.

Consistent with theory (Supplemental Material), the measured radial strain in the presence of off-resonance and T2* decay was dependent on the readout duration such that longer readouts underestimated radial strain (Figure 2B). In the worst simulated case, the measured radial strain was underestimated by 21% (absolute) compared to the reference. Measured circumferential strain in the presence of off-resonance and T2* decay was dependent on both the readout duration and the location of the measurement (Figure 2C). Longer readouts underestimated the magnitude of circumferential strain at the subendocardium while overestimating at the subepicardium. The magnitude of error was lower than that for radial strain; the largest error was 1.8% (absolute) in subendocardial circumferential strain during the worst simulated case. Both the direction of the errors in circumferential strain and their relative magnitude compared to errors in radial strain were consistent with theory. Similar simulated strain results were observed when the T2* and off-resonance were limited to a region of the myocardium and strain was measured from that region (Supplemental Material, Figure 1).

3.2 Participant DENSE Imaging

Compared to 1.9 ms readouts, magnitude images from 11.1 ms readouts showed blurring in the anterior and lateral segments of the left ventricle (Figure 3) at both 3.0 T and 1.5 T. Consistent with simulations, however, artifacts were not visually obvious in phase images (Figure 4). The phase images were only subtly different between acquisitions with 11.1 and 1.9 ms readouts. The degree of blurring in the magnitude images was diminished as the readout duration decreased (Figure 5). Global image quality was reduced as the readout duration increased (Figure 6).

3.3 Participant Radial Strain

At 3.0 T, global radial strain and several segmental radial strains were significantly correlated with the readout duration (Figure 7A). Among the anterior and lateral segments of the left ventricle, measured radial strain decreased between 0.90 and 2.12% for every

millisecond of readout duration. With a difference of 9.2 ms between the 11.1 and 1.9 ms readouts, those rates correspond to differences in measured radial strain of 8.3 and 19.5% (absolute), or 17 and 42% (relative to the strain from 1.9 ms readouts). There was no correlation in the inferior and inferoseptal segments. Summary strain results from the 1.9 and 11.1 ms readouts are reported in Table 2.

Similar results for radial strain were present at 1.5 T (Figure 7B). The measured radial strains in the anterior segments were significantly and negatively correlated with the readout duration while the inferior and inferoseptal segments were not correlated. In contrast to results at 3.0T, there was no significant correlation in the inferolateral segment or globally. Among the anterior segments, measured radial strain decreased between 1.03 and 2.13% per ms, which corresponds to differences of 9.5 and 19.6% (absolute), or 17 and 39% (relative), between the 11.1 and 1.9 ms readouts.

3.4 Participant Circumferential Strain

At 3.0 T, significant correlations between the readout duration and circumferential strain were found globally and in the anterior segments (Figure 8A). For the subendocardial layer of affected segments, the magnitude of the circumferential strain decreased by between 0.147 and 0.159% per millisecond, which correspond to differences of 1.4 and 1.5% (absolute), or 7% (relative) for both, between the 11.1 and 1.9 ms readouts. In the inferior segments, there were no significant correlations between circumferential strain and readout duration. At 1.5 T, there were few significant correlations between circumferential strain and the readout duration (Figure 8B). The sole significance was observed in the anterolateral segment. As with all reported strains in this study, no significant correlations were seen in the inferior or inferoseptal segments.

4. Discussion

Spiral cine DENSE is typically acquired with 6 interleaves and an 11.1 ms readout duration [6–8, 13–17]. The current study investigated the degree to which blurring affects measured cardiac strains at both 3.0 T and 1.5 T. Our primary findings included: 1) Computational simulations demonstrated that longer spiral readout durations in the presence of off-resonance and T2* decay yield blurred images, substantial reductions in measured radial strain, and mild errors in measured circumferential strain; 2) In participants, substantial blurring was apparent with 11.1 ms readouts compared to 1.9 ms readouts at both 3.0 T and 1.5 T; 3) the blurring was predominantly in the anterior and lateral segments of the left ventricle; 4) similar to the simulations, radial strain was underestimated by the 11.1 ms readouts, compared to the 1.9 ms readouts, at both field strengths and in the same segments where blurring was present; and 5) circumferential strain was less dependent on the readout duration, but was mildly underestimated by the 11.1 ms readout in the subendocardial layer at 3.0 T.

Spiral acquisitions are prone to blurring with longer readout durations due to phenomena such as off-resonance and T2* decay. Because blurring affects the entire complex signal, and not just the magnitude, measurements from quantitative phase contrast techniques like DENSE may depend on the amount of blurring. The theoretical relationship between

blurring and strain suggested that measured radial strain would be substantially reduced in the presence of blurring while the effect on circumferential strain would be lower in magnitude. Computational simulations of off-resonance and T2* decay resulted in blurred images and alterations in the measured strains that were consistent with this theory.

In participants, blurring was present with longer readout durations and had similar appearance between 3.0 T and 1.5 T. The anterior and lateral segments of the left ventricle were predominantly affected. This is consistent with the presence of the lung-heart interface as well as the presence of epicardial veins carrying deoxygenated blood [19]. Tissue-air interfaces and tissues with susceptibility differences are prone to generating off-resonance and T2* decay artifacts [19]. Global image quality declined as the readout duration was increased, consistent with the behavior of spirals in the presence of system non-idealities. The regional analysis of image quality was limited by the resolution of the images and the subsequent low number of pixels available within each cardiac segment. However, the general trend of declining image quality with increasing readout duration was observed in all segments at both field strengths. In addition, image quality in the inferior-septal segment was relatively preserved as the readout duration increased compared to the more rapid decline in image quality with increasing readout duration that was seen in other segments (Supplemental Material, Figure 2).

Radial strain was substantially underestimated – by up to 19.6 % (absolute) – with 11.1 ms readouts in the anterior and lateral segments at 3.0 T and in the anterior segments at 1.5 T compared to the 1.9 ms readouts. Notably, blurring was typically observed in these segments within the magnitude images. Subendocardial circumferential strain was also generally underestimated by the 11.1 ms readout, but to a lesser extent – up to 1.5 % (absolute), consistent with theory. Small differences were seen globally and in some anterior segments at 3.0 T. No differences in either radial or circumferential strain were seen in the inferior and inferoseptal segments, which was consistent with the lack of visual blurring artifacts in those regions.

To put the strain differences in context of the reproducibility of spiral cine DENSE, a previous study reported inter-test Bland-Altman limits of 13% and 2% for global radial and global circumferential strains, respectively [16]. The differences in strain between shortest and longest readout durations in the current study were on the order of the reported Bland-Altman limits. However, inter-test variability would not explain the consistent directionality, which was in the theorized direction (*e.g.* radial strain was consistently underestimated when using longer readout durations). Our results also suggest that phenomena such as off-resonance and T2* may contribute to inter-test variability due to their effects on measured strains and their possible variability between imaging sessions.

The strain values reported in this study (Table 2) are similar to those from previous studies. For the current study at 3.0 T and with 11.1 ms readouts, the global radial and midwall circumferential strains were $36 \pm 3\%$ and $-16 \pm 2\%$, respectively. At 1.5 T and with 11.1 ms readouts, the global radial and midwall circumferential strains were $42 \pm 9\%$ and $-16 \pm 1\%$, respectively. One study with 6 interleaves (11.1 ms readout) conducted at both 3.0 T and 1.5 T reported global strain results that are within the above limits of agreement compared to the

current study [7]. At 3.0 T, they reported $28 \pm 7\%$ and $-18 \pm 2\%$ for radial and circumferential strain, respectively; at 1.5 T, they reported $42 \pm 10\%$ and $-18 \pm 1\%$ for radial and circumferential strain, respectively [7]. The strains from 11.1 ms readouts in the current study also compare well with results from another study with 6 interleaves at 1.5 T [13]. No previous studies of readout durations down to 1.9 ms exist for comparison.

Validation of the spiral cine DENSE sequence with 6 interleaves and 11.1 ms readout duration has previously been performed in several ways: radial and shear strain comparisons in a non-physiologic deforming phantom at 1.5 T [13], radial and circumferential strain comparisons to results from tagged MRI at 1.5 T [13], and a comparison of displacement error at 3.0 T versus 1.5 T [7]. While these techniques were appropriate, they did have limitations that restricted their abilities to detect the effects that were evaluated in the current study. The phantom study likely did not reproduce field inhomogeneities that are present due to human anatomy and it assessed non-physiologic motion [13]. The comparisons with strain results from tagged MRI were subject to any errors or variability associated with tagged images and their image processing [13]. The comparison of DENSE displacement error between 3.0 T and 1.5 T utilized the acquisitions at 1.5 T as a reference and found no differences between displacement errors at 3.0 T compared to 1.5 T [7]. This suggested that spiral cine DENSE at 3.0 T was not demonstrably worse than spiral cine DENSE at 1.5 T, but it could not detect any errors associated with DENSE at 1.5 T. Hence, the present findings do not invalidate these previous comparisons, but do identify important sensitivities in the spiral DENSE acquisition that were not previously appreciated.

4.1 Implications

Although the blurring effect of long spiral readouts in the presence of system non-idealities is well understood, the implications of this blurring on phase-based measurements has not been systematically investigated. The results of the current study make it clear that applying a single set of acquisition parameters across studies with different aims is inappropriate. Users of spiral cine DENSE should therefore carefully tune the balance between scan time and the measurement requirements of a particular study.

For instance, the typical 6-interleaves, 11.1 ms acquisition is likely sufficient for attempting to identify myocardial dysfunction based on reduced circumferential strain since the dependence of circumferential strain on readout duration was small. This is largely due to the relative insensitivity of circumferential strain to small differences in measured displacement as theorized. While this insensitivity is beneficial when displacement differences are due to small errors from blurring, it may hinder the detection of small differences that arise from actual subclinical disease.

However, for radial strain, the dependence on readout duration was much stronger, particularly in the anterior and lateral segments, which is consistent with the theory that radial strain is very sensitive to small differences in measured displacement. For studies with a specific interest in segmental radial strains, care should be taken when choosing protocol parameters, as the relationship between scan duration and measured strain varies across segments. Similarly, for studies on the detailed structure, deformation, and tissue properties of the left ventricle, 11.1 ms readouts are not recommended as the blurring in the magnitude

images compromises the extracted geometry of the ventricle while the phase images yield dampened strains.

Future technical developments of spiral cine DENSE may allow for the realization of the quality of the 1.9 ms readouts without requiring many heartbeats of acquisition time. It may be possible to replace the linear corrections for field inhomogeneities with more advanced algorithms [26–29]. Recent advancements have also included zonal excitation around the heart ([30]), which allows for a reduced field of view, and both parallel imaging and compressed sensing ([31]), which allow for undersampling of k-space data. The combination of these advancements is a promising future direction for accelerating the spiral cine DENSE acquisition [32], but it may be that the gains achieved by new techniques must be traded for improved quality and repeatability rather than simply accelerating the DENSE acquisition. The results of the current study motivate continued development in this area.

While the current study utilized spiral cine DENSE, other spiral phase contrast techniques exist to measure blood and tissue velocities [1, 11, 12]. Readout durations between 11.75 and 14 ms have been reported [1, 11, 12]. Based on the results of this study, those readout durations may yield velocity-encoded phase images that are compromised by their readout duration. In particular, identical problems would arise if spatial derivatives of the velocity-encoded images were used to calculate shear or strain rates. For other applications, including first pass perfusion and balanced steady state free precession imaging of the heart, shorter spiral readout durations between 1.5 and 7.1 ms have been used [33–35].

4.2 Limitations

No additional imaging technique was acquired as an objective reference (such as myocardial tagging). However, the theoretical relationship between blurring and cardiac strains was considered first in detail. Then, computational simulations demonstrated the potential for both blurring and underestimation of strain with a spiral cine DENSE sequence in the presence of common phenomena such as off-resonance and T2* decay. Lastly, the acquired imaging data was then sufficient to corroborate the simulations and fulfill the purpose of the study, which was to evaluate the dependence of both blurring artifacts and measured strains on the spiral cine DENSE readout duration.

Acquisitions with more interleaves were necessarily longer (*i.e.* required more heart beats), which allowed more time for physiologic changes that could have their own effect on image quality and measured strains. However, the artifacts found in this study were present in acquisitions with fewer heart beats (long readout durations). It would have been possible to assess a limited number of different readout durations without large changes in acquisition time, however differences in spatial resolution, temporal resolution, and SNR would have been required, which would have their own independent effects on measured peak strains. The chosen study design allowed for the same spatial and temporal resolutions, as well as the same SNR, between the different acquisitions.

With the small sample size used in this study, subtle differences in cardiac strains may have been missed in the myocardial segments that were least affected by the readout duration.

However, the current sample size was sufficiently powered for demonstrating the dependence of several measurements of cardiac strains on the spiral readout duration.

4.3 Conclusion

Blurring due to a long readout duration is present in spiral cine DENSE images acquired at both 3.0 T and 1.5 T using the typical 6-interleaves acquisition with an 11.1 ms readout duration. These artifacts yield substantially reduced radial strains and mildly reduced circumferential strains in short-axis views of the left ventricle. Reducing the readout duration diminishes the presence of these artifacts. Clinical studies using spiral cine DENSE should consider these limitations, while future technical advances may need to leverage accelerated techniques to improve the robustness and accuracy of the DENSE acquisition rather than focusing solely on reduced acquisition time.

Supplementary Material

Refer to Web version on PubMed Central for supplementary material.

Acknowledgments

Funding

This work was supported by a National Institutes of Health (NIH) Director's Early Independence Award (DP5 OD-012132), NIH grant number T32 HL-072743, and NIH grant number UL1TR000117 from the National Center for Research Resources and the National Center for Advancing Translational Sciences. The content is solely the responsibility of the authors and does not necessarily represent the official views of NIH.

Abbreviations

DENSE	displacement encoding with stimulated echoes
MR	magnetic resonance
PC	phase contrast
SNR	signal to noise ratio

References

1. Simpson R, Keegan J, Gatehouse P, Hansen M, Firmin D. Spiral tissue phase velocity mapping in a breath-hold with non-cartesian SENSE. *Magn Reson Med*. 2014;72:659–68. doi:10.1002/mrm.24971. [PubMed: 24123135]
2. Kim D, Gilson WD, Kramer CM, Epstein FH. Myocardial tissue tracking with two-dimensional cine displacement-encoded MR imaging: development and initial evaluation. *Radiology*. 2004;230:862–71. [PubMed: 14739307]
3. Aletras AH, Ding S, Balaban RS, Wen H. DENSE: displacement encoding with stimulated echoes in cardiac functional MRI. *J Magn Reson*. 1999;137:247–52. doi:10.1006/jmre.1998.1676. [PubMed: 10053155]
4. Stanton T, Leano R, Marwick TH. Prediction of all-cause mortality from global longitudinal speckle strain: comparison with ejection fraction and wall motion scoring. *Circ Cardiovasc Imaging*. 2009;2:356–64. [PubMed: 19808623]

5. Choi EY, Rosen BD, Fernandes VR, Yan RT, Yoneyama K, Donekal S, et al. Prognostic value of myocardial circumferential strain for incident heart failure and cardiovascular events in asymptomatic individuals: the Multi-Ethnic Study of Atherosclerosis. *Eur Hear J*. 2013;34:2354–61.
6. Bilchick KC, Kuruvilla S, Hamirani YS, Ramachandran R, Clarke SA, Parker KM, et al. Impact of mechanical activation, scar, and electrical timing on cardiac resynchronization therapy response and clinical outcomes. *J Am Coll Cardiol*. 2014;63:1657–66. [PubMed: 24583155]
7. Wehner GJ, Suever JD, Haggerty CM, Jing L, Powell DK, Hamlet SM, et al. Validation of in vivo 2D displacements from spiral cine DENSE at 3T. *J Cardiovasc Magn Reson*. 2015;17:5. [PubMed: 25634468]
8. Zhong X, Spottiswoode BS, Meyer CH, Kramer CM, Epstein FH. Imaging three-dimensional myocardial mechanics using navigator-gated volumetric spiral cine DENSE MRI. *Magn Reson Med*. 2010;64:1089–97. doi:10.1002/mrm.22503. [PubMed: 20574967]
9. Delattre BMA, Heidemann RM, Crowe LA, Vallée J-P, Hyacinthe J-N. Spiral demystified. *Magn Reson Imaging*. 2010;28:862–81. doi:10.1016/j.mri.2010.03.036. [PubMed: 20409660]
10. Fielden SW, Meyer CH. A simple acquisition strategy to avoid off-resonance blurring in spiral imaging with redundant spiral-in/out k-space trajectories. *Magn Reson Med*. 2015;73:704–10. [PubMed: 24604539]
11. Simpson R, Keegan J, Firmin D. Efficient and reproducible high resolution spiral myocardial phase velocity mapping of the entire cardiac cycle. *J Cardiovasc Magn Reson*. 2013;15:34. [PubMed: 23587250]
12. Keegan J, Raphael CE, Parker K, Simpson RM, Strain S, de Silva R, et al. Validation of high temporal resolution spiral phase velocity mapping of temporal patterns of left and right coronary artery blood flow against Doppler guidewire. *J Cardiovasc Magn Reson*. 2015;17:85. [PubMed: 26428627]
13. Young AA, Li B, Kirton RS, Cowan BR. Generalized spatiotemporal myocardial strain analysis for DENSE and SPAMM imaging. *Magn Reson Med*. 2012;67:1590–9. [PubMed: 22135133]
14. Budge LP, Helms AS, Salerno M, Kramer CM, Epstein FH, Bilchick KC. MR cine DENSE dyssynchrony parameters for the evaluation of heart failure: comparison with myocardial tissue tagging. *JACC Cardiovasc Imaging*. 2012;5:789–97. [PubMed: 22897992]
15. Auger DA, Zhong X, Epstein FH, Spottiswoode BS. Mapping right ventricular myocardial mechanics using 3D cine DENSE cardiovascular magnetic resonance. *J Cardiovasc Magn Reson*. 2012;14:4. [PubMed: 22236389]
16. Wehner GJ, Grabau JD, Suever JD, Haggerty CM, Jing L, Powell DK, et al. 2D cine DENSE with low encoding frequencies accurately quantifies cardiac mechanics with improved image characteristics. *J Cardiovasc Magn Reson*. 2015;17:93. [PubMed: 26538111]
17. Suever JD, Wehner GJ, Haggerty CM, Jing L, Hamlet SM, Binkley CM, et al. Simplified post processing of cine DENSE cardiovascular magnetic resonance for quantification of cardiac mechanics. *J Cardiovasc Magn Reson*. 2014;16:94. [PubMed: 25430079]
18. Dong SJ, MacGregor JH, Crawley AP, McVeigh E, Belenkie I, Smith ER, et al. Left ventricular wall thickness and regional systolic function in patients with hypertrophic cardiomyopathy. A three-dimensional tagged magnetic resonance imaging study. *Circulation*. 1994;90:1200–9. [PubMed: 8087929]
19. Reeder SB, Faranesh AZ, Boxerman JL, McVeigh ER. In vivo measurement of T2(*) and field inhomogeneity maps in the human heart at 1.5 T. *Magn Reson Med*. 1998;39:988–98. [PubMed: 9621923]
20. Zhong X, Helm PA, Epstein FH. Balanced multipoint displacement encoding for DENSE MRI. *Magn Reson Med*. 2009;61:981–8. [PubMed: 19189288]
21. Zhong X, Spottiswoode BS, Cowart EA, Gilson WD, Epstein FH. Selective suppression of artifact-generating echoes in cine DENSE using through-plane dephasing. *Magn Reson Med*. 2006;56:1126–31. [PubMed: 17036303]
22. Jackson JI, Meyer CH, Nishimura DG, Macovski A. Selection of a convolution function for Fourier inversion using gridding. *IEEE Trans Med Imaging*. 1991;10:473–8. [PubMed: 18222850]

23. Wang Z, Bovik AC, Sheikh HR, Simoncelli EP. Image Quality Assessment: From Error Visibility to Structural Similarity. *IEEE Trans Image Process.* 2004;13:600–12. doi:10.1109/TIP.2003.819861. [PubMed: 15376593]
24. Spottiswoode BS, Zhong X, Hess AT, Kramer CM, Meintjes EM, Mayosi BM, et al. Tracking myocardial motion from cine DENSE images using spatiotemporal phase unwrapping and temporal fitting. *IEEE Trans Med Imaging.* 2007;26:15–30. [PubMed: 17243581]
25. Gilliam AD, Suever JD. *DENSEanalysis.* 2016.
26. Noll DC, Meyer CH, Pauly JM, Nishimura DG, Macovski A. A homogeneity correction method for magnetic resonance imaging with time-varying gradients. *IEEE Trans Med Imaging.* 1991;10:629–37. doi:10.1109/42.108599. [PubMed: 18222870]
27. Moriguchi H, Dale BM, Lewin JS, Duerk JL. Block regional off-resonance correction (BRORC): A fast and effective deblurring method for spiral imaging. *Magn Reson Med.* 2003;50:643–8. [PubMed: 12939775]
28. Chen W, Meyer CH. Semiautomatic off-resonance correction in spiral imaging. *Magn Reson Med.* 2008;59:1212–9. doi:10.1002/mrm.21599. [PubMed: 18429033]
29. Sutton BP, Noll DC, Fessler JA. Fast, iterative image reconstruction for MRI in the presence of field inhomogeneities. *IEEE Trans Med Imaging.* 2003;22:178–88. [PubMed: 12715994]
30. Scott AD, Tayal U, Nielles-Vallespin S, Ferreira P, Zhong X, Epstein FH, et al. Accelerating cine DENSE using a zonal excitation. *J Cardiovasc Magn Reson.* 2016;18 Suppl 1:O50.
31. Chen X, Yang Y, Salerno M, Meyer CH, Epstein FH. Accelerated cine DENSE MRI using compressed sensing and parallel imaging. *J Cardiovasc Magn Reson.* 2014;16 Suppl 1:W16.
32. Chen X, Yang Y, Cai X, Auger DA, Meyer CH, Salerno M, et al. Accelerated two-dimensional cine DENSE cardiovascular magnetic resonance using compressed sensing and parallel imaging. *J Cardiovasc Magn Reson.* 2016;18:38. doi:10.1186/s12968-016-0253-2. [PubMed: 27301487]
33. Shin T, Nayak KS, Santos JM, Nishimura DG, Hu BS, McConnell MV. Three-dimensional first-pass myocardial perfusion MRI using a stack-of-spirals acquisition. *Magn Reson Med.* 2013;69:839–44. [PubMed: 22556062]
34. Salerno M, Sica C, Kramer CM, Meyer CH. Improved first-pass spiral myocardial perfusion imaging with variable density trajectories. *Magn Reson Med.* 2013;70:1369–79. [PubMed: 23280884]
35. Feng X, Salerno M, Kramer CM, Meyer CH. Non-Cartesian balanced steady-state free precession pulse sequences for real-time cardiac MRI. *Magn Reson Med.* 2015;00:1–10.

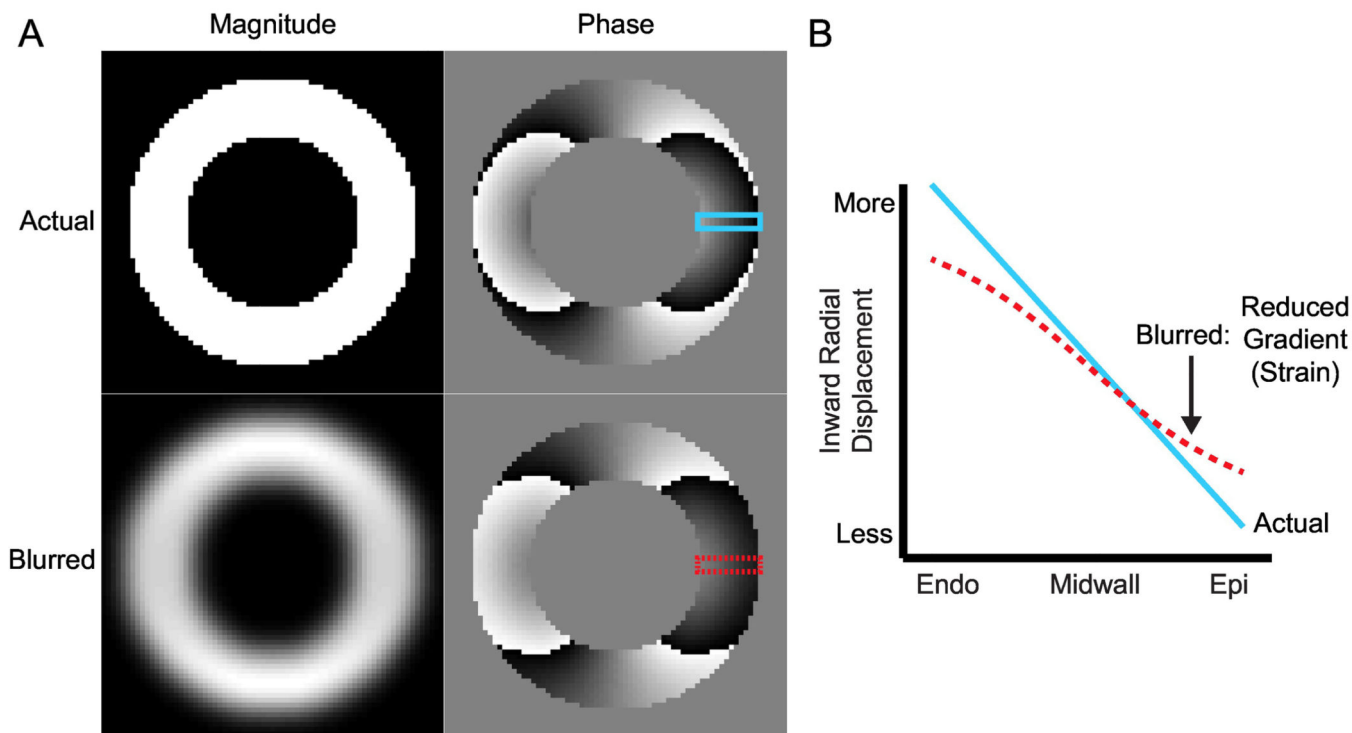


Figure 1. Illustration of blurring that causes a reduction in the observed radial displacement gradient.

(A) In the short-axis view, the left ventricle can be approximated as a ring of tissue. The top row contains the magnitude and phase components from a simulated, complex DENSE image. Displacement in the x-direction has been encoded into the phase. The bottom row contains the results of blurring the complex image with a Gaussian filter. The magnitude image is clearly blurred while the differences in the phase image are visually subtle. (B) The prescribed gradient in displacement across the left ventricular wall is shown as the blue line and was taken from the top phase image. The dashed red line is the displacement gradient across the wall in the blurred phase image. There is a clear reduction in the measured displacement gradient (strain) across the wall in the presence of blurring. Endo: endocardial boundary; Epi: epicardial boundary.

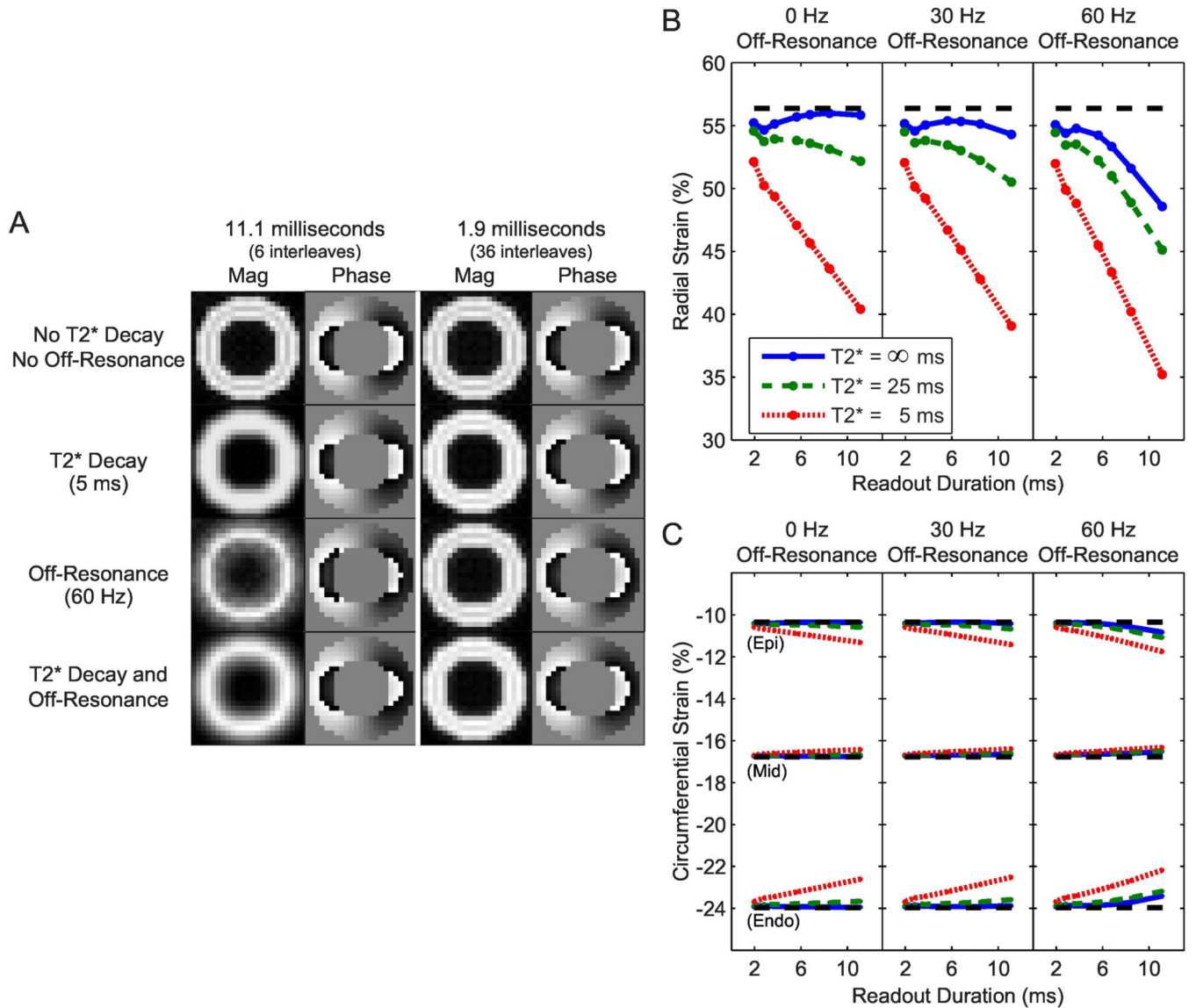


Figure 2. Simulations of longer readout durations in the presence of off-resonance and T2* decay yield blurred images and erroneous strain measurements.

A) Simulations with longer readout durations were more susceptible to blurring from off-resonance and T2* decay. B) Radial strain was underestimated as the readout duration increased in the presence of off-resonance and T2* decay. The dashed line represents the measured strain from the reference simulation. C) Measured circumferential strain was also altered with longer readout durations in the presence of off-resonance and T2* decay, however the magnitude was less than that of radial strain and the direction was dependent on the location of the measurement (Epi: epicardium; Mid: midwall; Endo: endocardium).

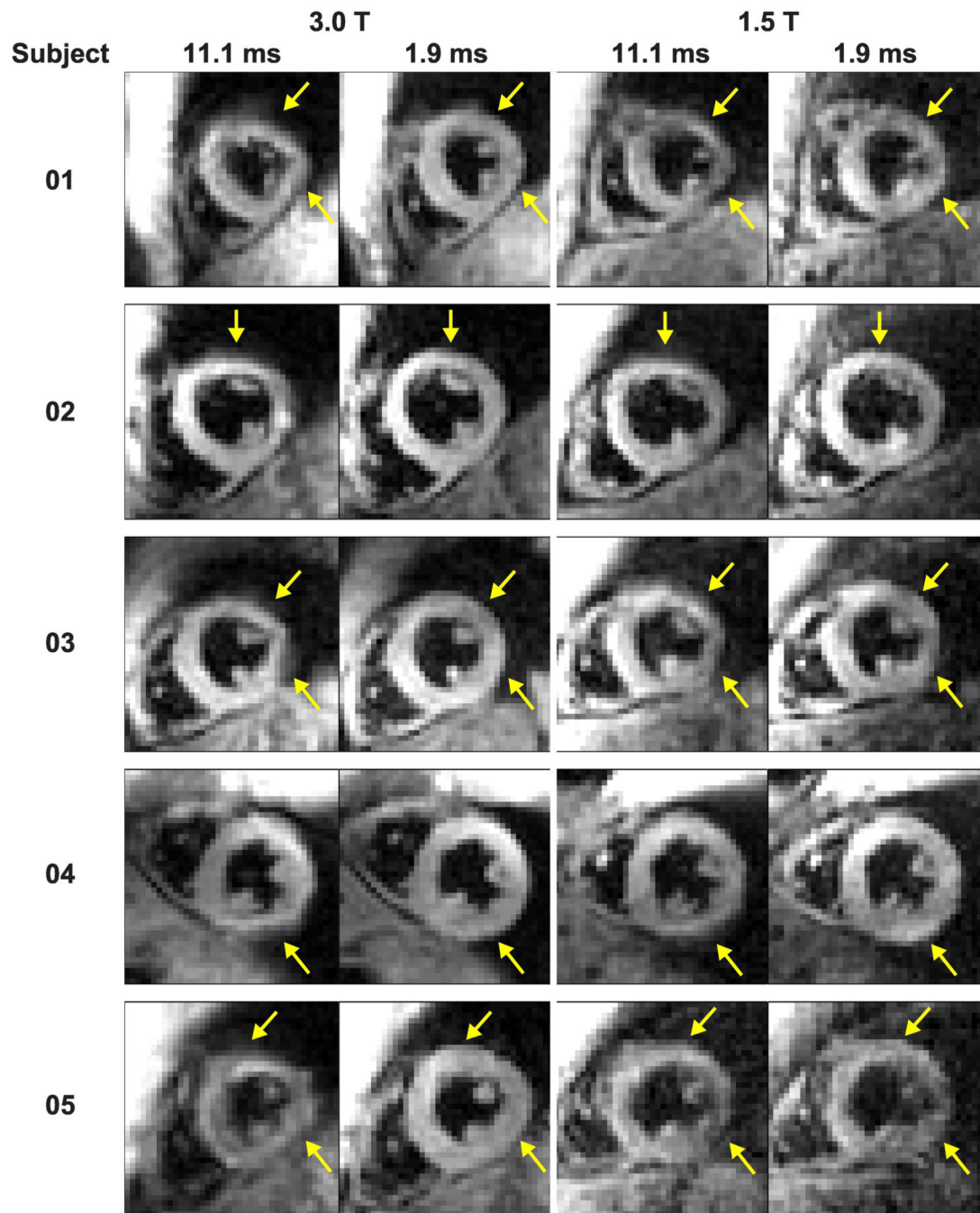


Figure 3. Acquisitions with 11.1 ms readouts demonstrated blurring in all subjects compared to 1.9 ms readouts.

The artifacts in the anterior and lateral walls of the left ventricle were variable between the subjects. However, within each subject, the artifacts were similar in location and appearance at 3.0 T and 1.5 T.

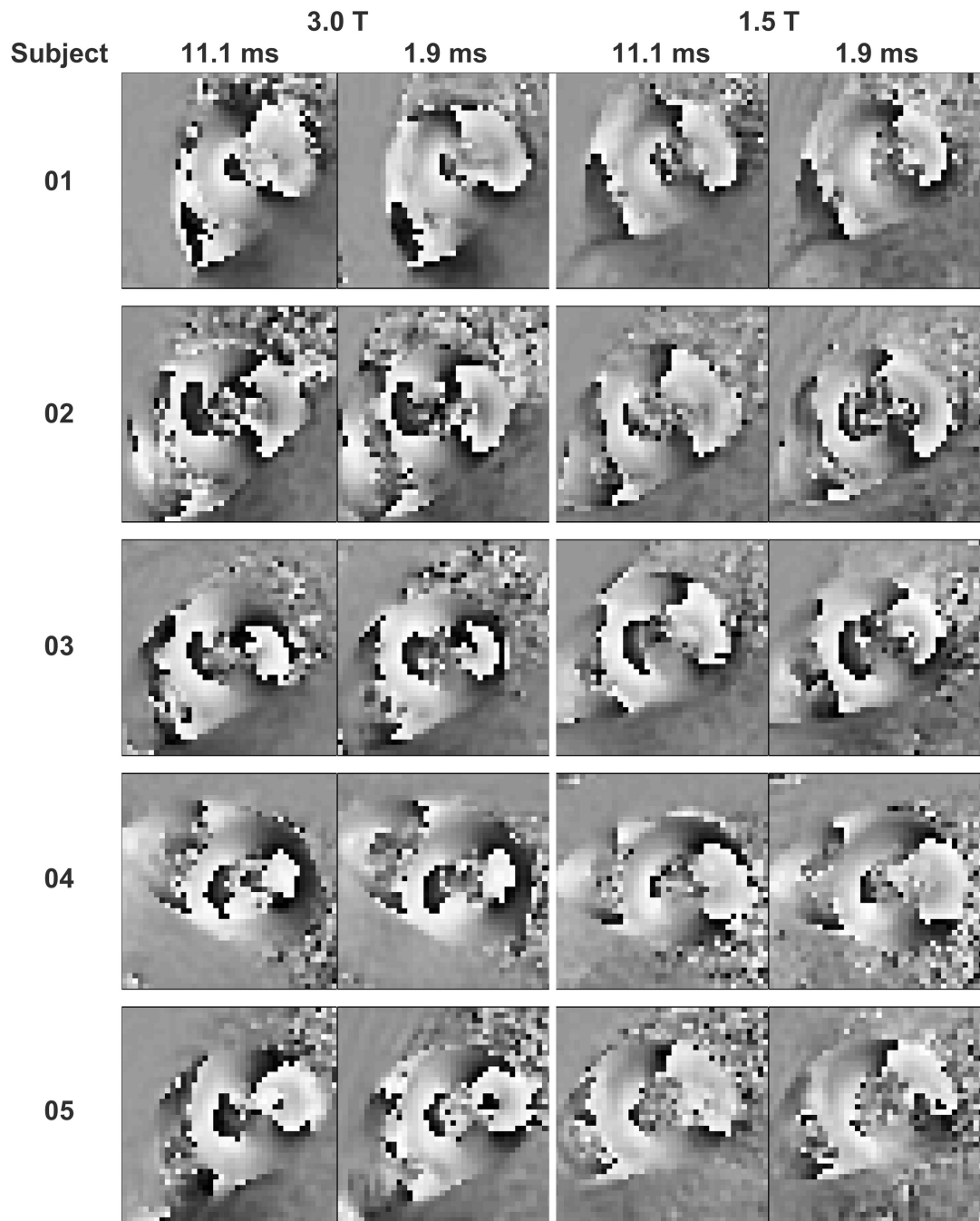


Figure 4. Phase images with displacement encoded in the x-direction were visually similar between acquisitions with 11.1 and 1.9 ms readouts. Blurring artifacts were not visually obvious in the phase images from 11.1 ms readouts.

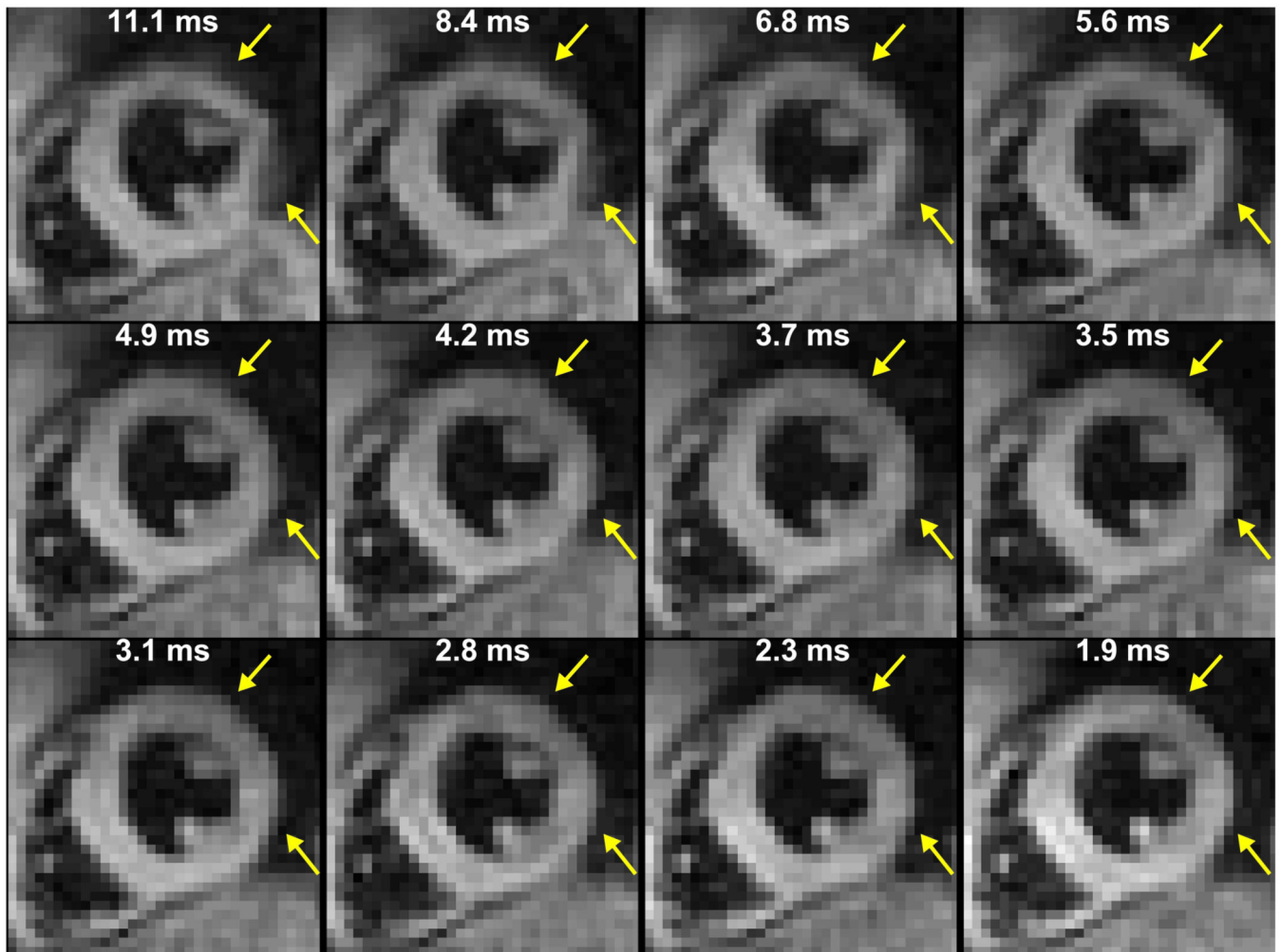


Figure 5. Blurring was diminished with decreasing readout duration.

The white text indicates the readout duration. In this representative subject at 3.0 T, blurring was present in the anterior and lateral segments of the left ventricle with 11.1 ms readouts. The artifacts become less severe as the readout duration is shortened.

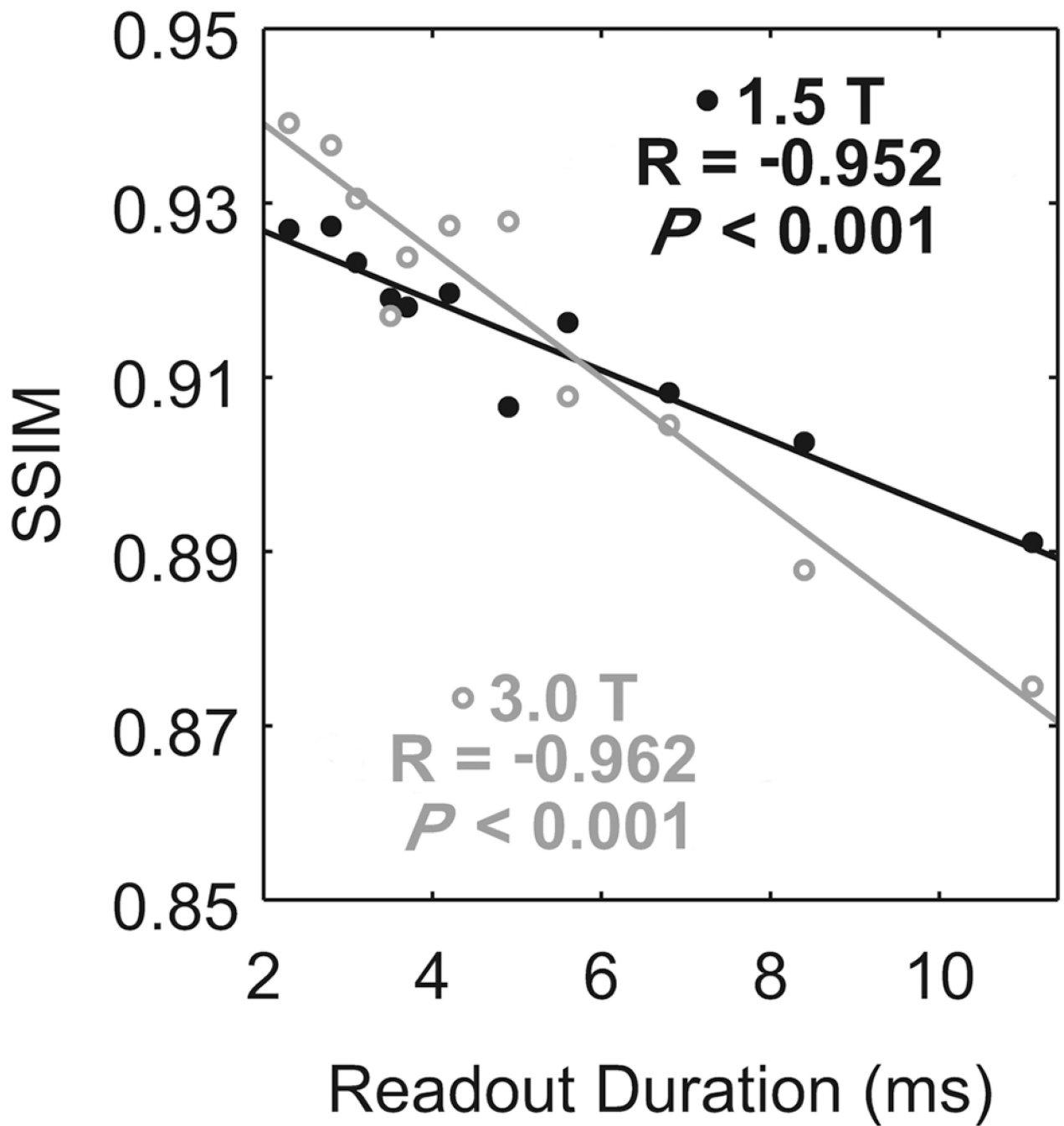


Figure 6. Image quality was diminished with increasing readout duration.

The mean of the subjects is represented either by closed, black circles (1.5 T) or by open, gray circles (3.0 T). The solid lines are the linear fits to the corresponding means. At both field strengths, global image quality was significantly correlated with the readout duration.

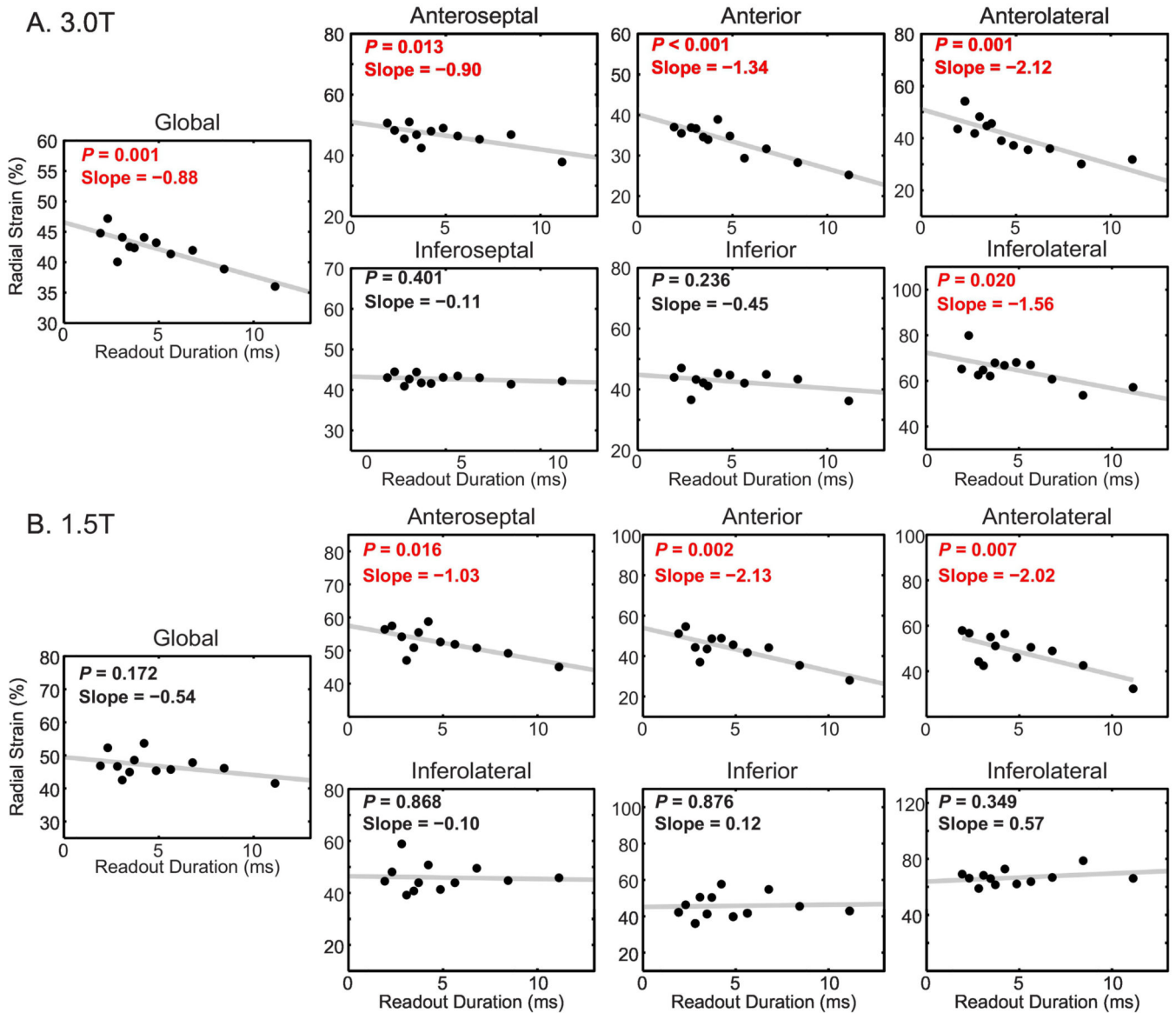


Figure 7. Radial strain was significantly correlated with the readout duration at both 3.0 and 1.5 T.

In each plot, the mean of the subjects is represented by the black points. The gray line is the linear fit to the mean of the subjects. Red text denotes statistical significance. Slope is reported in units of %/ms. **A)** At 3.0 T, anterior and lateral radial strains, as well as global radial strain, were significantly correlated with the number of interleaves. **B)** At 1.5 T, anterior radial strains were significantly correlated with the readout duration. However, unlike the results at 3.0 T, inferolateral and global radial strains were not significantly correlated.

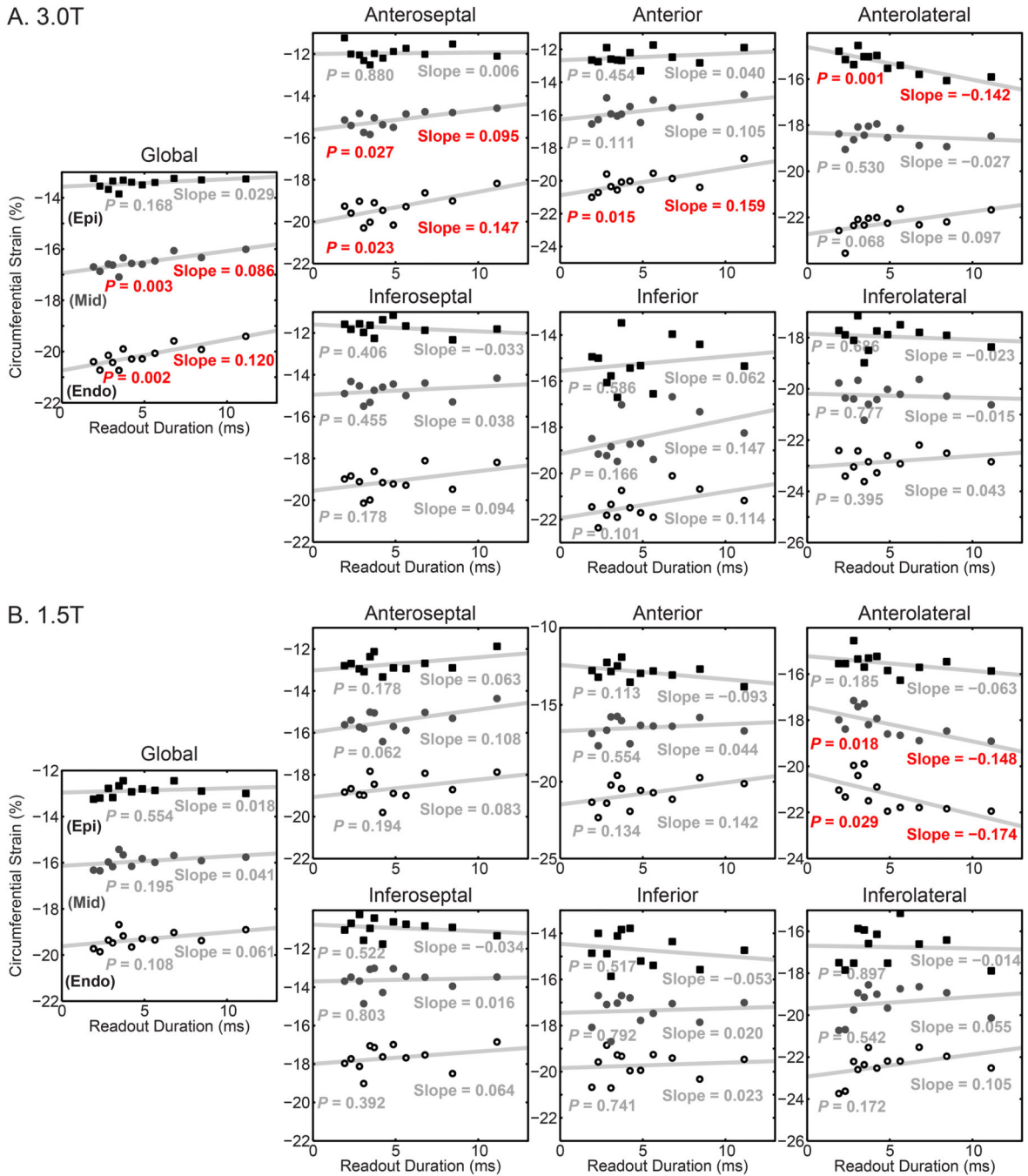


Figure 8. Circumferential strains were significantly correlated with the readout duration at 3.0 T. In each plot, the mean of the subjects is represented by the points. The gray line is the linear fit to the mean of the subjects. Red text denotes statistical significance. Circumferential strain was reported for the subepicardium (Epi – closed squares), midwall (Mid – closed circles), and subendocardium (Endo – open circles). Slope is reported in units of %/ms. **A)** At 3.0 T, global and anterior circumferential strains were significantly correlated with

readout duration **B)** At 1.5 T, only the circumferential strains in the anterolateral segment correlated with the readout duration.

Author Manuscript

Author Manuscript

Author Manuscript

Author Manuscript

Table 1.

Spiral DENSE readout parameters

Number of Interleaves	Readout Samples	Readout Duration (ms)	Number of Heart Beats
6	2784	11.1	20
8	2112	8.4	26
10	1696	6.8	32
12	1408	5.6	38
14	1216	4.9	44
16	1056	4.2	50
18	928	3.7	56
20	864	3.5	62
22	768	3.1	68
24	704	2.8	74
30	576	2.3	92
36	480	1.9	110

Author Manuscript

Author Manuscript

Author Manuscript

Author Manuscript

Table 2.Mean (\pm standard deviation) strains from the 11.1 and 1.9 ms readout durations

<i>Readout Duration(ms):</i>	<i>Radial Strain (%)</i>		<i>Circumferential Strain (%)</i>					
	<i>11.1</i>	<i>1.9</i>	<i>Subendocardial</i>		<i>Midwall</i>		<i>Subepicardial</i>	
			<i>11.1</i>	<i>1.9</i>	<i>11.1</i>	<i>1.9</i>	<i>11.1</i>	<i>1.9</i>
3.0T								
<i>Global</i>	36 \pm 3	45 \pm 4	-19 \pm 1	-20 \pm 1	-16 \pm 2	-17 \pm 2	-13 \pm 2	-13 \pm 2
<i>Anterior</i>	25 \pm 9	37 \pm 6	-19 \pm 1	-21 \pm 1	-15 \pm 1	-17 \pm 2	-12 \pm 1	-13 \pm 2
<i>Anteroseptal</i>	38 \pm 13	51 \pm 9	-18 \pm 4	-19 \pm 3	-15 \pm 4	-15 \pm 2	-12 \pm 2	-11 \pm 3
<i>Inferoseptal</i>	42 \pm 10	43 \pm 9	-18 \pm 4	-19 \pm 4	-14 \pm 4	-15 \pm 3	-12 \pm 4	-12 \pm 4
<i>Inferior</i>	36 \pm 7	44 \pm 16	-21 \pm 3	-21 \pm 3	-18 \pm 4	-18 \pm 2	-15 \pm 4	-15 \pm 3
<i>Inferolateral</i>	57 \pm 26	65 \pm 12	-23 \pm 4	-22 \pm 1	-21 \pm 3	-20 \pm 2	-18 \pm 3	-18 \pm 1
<i>Anterolateral</i>	32 \pm 7	44 \pm 10	-22 \pm 3	-23 \pm 2	-18 \pm 3	-18 \pm 3	-16 \pm 3	-15 \pm 3
1.5T								
<i>Global</i>	42 \pm 9	47 \pm 12	-19 \pm 2	-20 \pm 3	-16 \pm 1	-16 \pm 2	-13 \pm 2	-13 \pm 2
<i>Anterior</i>	28 \pm 7	51 \pm 12	-20 \pm 2	-21 \pm 1	-17 \pm 2	-17 \pm 2	-14 \pm 3	-13 \pm 2
<i>Anteroseptal</i>	45 \pm 3	56 \pm 7	-18 \pm 2	-19 \pm 4	-14 \pm 1	-16 \pm 3	-12 \pm 1	-13 \pm 2
<i>Inferoseptal</i>	46 \pm 10	45 \pm 9	-17 \pm 2	-18 \pm 4	-13 \pm 1	-14 \pm 3	-11 \pm 2	-11 \pm 2
<i>Inferior</i>	43 \pm 23	42 \pm 17	-19 \pm 2	-21 \pm 4	-17 \pm 2	-18 \pm 4	-15 \pm 2	-15 \pm 4
<i>Inferolateral</i>	66 \pm 27	69 \pm 31	-23 \pm 2	-24 \pm 2	-20 \pm 2	-21 \pm 1	-18 \pm 1	-17 \pm 1
<i>Anterolateral</i>	32 \pm 10	58 \pm 22	-22 \pm 2	-21 \pm 4	-19 \pm 3	-18 \pm 4	-16 \pm 3	-16 \pm 3